

# Inhibitory growth evaluation and apoptosis induction in MCF-7 cancer cells by new 5-aryl-2-butylthio-1,3,4-oxadiazole derivatives

Rashmin Khanam<sup>1</sup> · Kamal Ahmad<sup>1</sup> · Iram I. Hejazi<sup>1</sup> · Ibrar A. Siddique<sup>2</sup> · Vikash Kumar<sup>2</sup> · Abdul Roouf Bhat<sup>3</sup> · Amir Azam<sup>4</sup> · Fareeda Athar<sup>1</sup> 

Received: 14 March 2017 / Accepted: 3 August 2017  
© Springer-Verlag GmbH Germany 2017

## Abstract

**Background** Cancer has become one of the global health issues and it is the life-threatening disease characterized by unrestrained growth of cells. Despite various advances being adopted by chemotherapeutic management, the use of the current anticancer drugs such as Doxorubicin, Asparaginase, Methotrexate, Vincristine remains limited due to high toxicity, side effects and developing drug resistance. Apoptosis is a crucial cellular process and improper regulation of apoptotic signaling pathways may lead to cancer formation. Subsequently, the synthesis of effective chemotherapeutic agents that can induce apoptosis in tumor cell has emerged as a significant approach in cancer drug discovery.

**Methods** The goal of this work is to develop a potential antitumor agent exerting significant inhibitory effects on cancer cell and low cytotoxicity, for which we focused on the structural features of 1,3,4-oxadiazoles as it a privileged scaffold in modern medicinal chemistry and have the ability to inhibit growth factors, enzymes and kinases potentially

involved in the attainment of cellular immortality and carcinogenesis.

**Result** In vitro MTT screening assay showed the compound 5-aminophenyl-2-butylthio-1,3,4-oxadiazole (**5e**) showing the highest inhibitory effect against MCF-7 cancer cell with IC<sub>50</sub> value 10.05 ± 1.08 μM while it is much safer and less toxic on normal cell line (HEK-293). The dose-dependent treatment of MCF-7 cells with **5e** resulted in inhibition of cell migration in the wound healing assay. The flow-cytometry analysis showed the cells arrested in G<sub>0</sub>/G<sub>1</sub> phase of the cell cycle. Compound **5e** induced apoptosis of MCF-7 cells was characterized using DAPI staining and Annexin V-PE/7-AAD dual binding assay. Reduction of NBT by compound **5e** showed a reduced generation of ROS. Western blotting studies showed high activation of apoptotic protein Caspase3 and decrease in expression of anti-apoptotic protein BCL-2.

**Conclusion** Based on the results of in vitro studies, it could be concluded that compound **5e** showed a significant inhibitory growth effect on MCF-7 cells and have the potential to be developed as lead molecule and further structural modifications may result in promising new anticancer agents.

**Electronic supplementary material** The online version of this article (doi:10.1007/s00280-017-3414-6) contains supplementary material, which is available to authorized users.

✉ Abdul Roouf Bhat  
abroouf@gmail.com

✉ Fareeda Athar  
fathar@jmi.ac.in

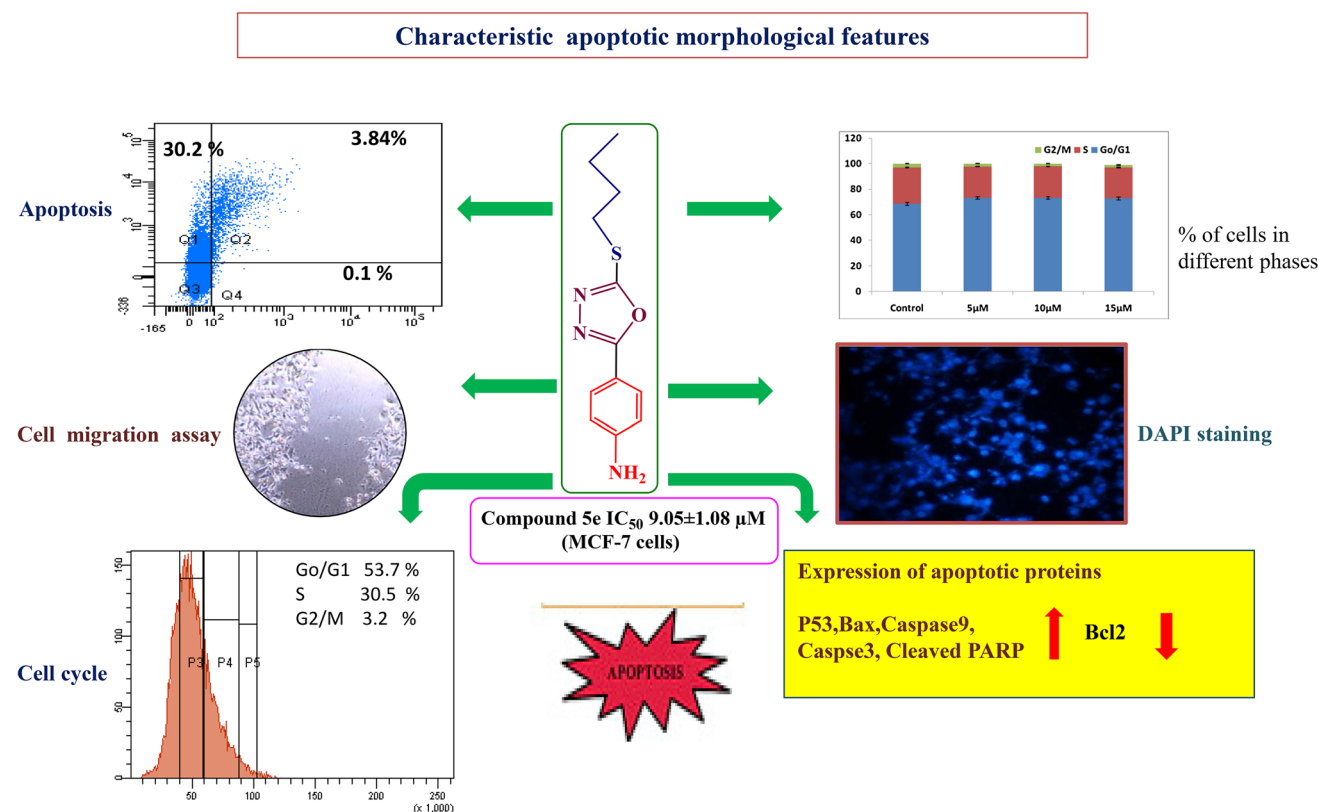
<sup>1</sup> Centre for Interdisciplinary Research in Basic Sciences, Jamia Millia Islamia, New Delhi 110025, India

<sup>2</sup> National Institute of Immunology, New Delhi 110067, India

<sup>3</sup> Department of Chemistry, Sri Pratap College, Cluster University, Srinagar 190001, India

<sup>4</sup> Department of Chemistry, Jamia Millia Islamia, New Delhi 110025, India

## Graphical abstract



**Keywords** 1,3,4-Oxadiazole derivatives · Apoptosis · Inhibition growth assay · Drug-like properties

## Introduction

Cancer has become one of the global health issues arising various clinical challenges with increasing frequency every year [1]. It is the life threatening disease characterized with unrestrained growth of cells. It also invades to other body parts and ranked as most deadly health problem after cardiovascular diseases [2]. Despite various advances being adopted by chemotherapeutic management, the use of the available anticancer drugs such as Doxorubicin, Asparaginase, Methotrexate, Vincristine, Mercaptopurine remains limited due to high toxicity, side effects and developing drug resistance [3]. Thus, there is need to identify a novel drug that can exhibit effective anticancer activity with minimum toxicity and lesser side effects. Antitumor agents act by stimulating apoptosis pathways leading to cell death [4]. Apoptosis is a crucial cellular process which plays a prominent role in governing growth of tissues and homeostasis [5]. The improper regulation of apoptotic signaling pathways has resulted in many ailments including cancer [6]. Subsequently, the synthesis of effective chemotherapeutic agents

that can induce apoptosis in tumor cell has emerged as a significant approach in cancer drug discovery [1, 7].

In the attempt of finding effective anticancer agents, many constructive efforts have been made on the development of heterocyclic moieties, depending on their structural framework. 1,3,4-oxadiazole is a privileged scaffold in modern medicinal chemistry and is an attractive pharmacophore for the development of new anticancer agents due to its wide spectrum and ability towards numerous biological targets [8]. The antitumor and cytotoxic potency of 1,3,4-oxadiazole derivatives (Fig. 1) are generally related to their ability to inhibit growth factors, enzymes and kinases potentially involved in the attainment of cellular immortality and carcinogenesis such as telomerase [9], HDAC [10], MetAP2, TS [11], GSK3 [12], FAK [13], VEGF [14] and EGFR [15]. Zibotentan (ZD4045) is an anticancer drug present in late clinical trial containing 1,3,4-oxadiazole nucleus, which has made the moiety more attractive for anticancer drug discovery [16]. The presence of an acyl or alkyl linkage on 1,3,4-oxadiazoles enhances their biological profile [17] and also substitution at C-2 of 1,3,4-oxadiazoles with *n*-butyl chain improves binding with various receptors [18].

Therefore, in the quest of developing a potential antitumor agent, we focused on the structural features of 1,3,4-oxadiazoles with the aim of synthesizing new small molecule exerting anti-proliferation effects on certain human cancer

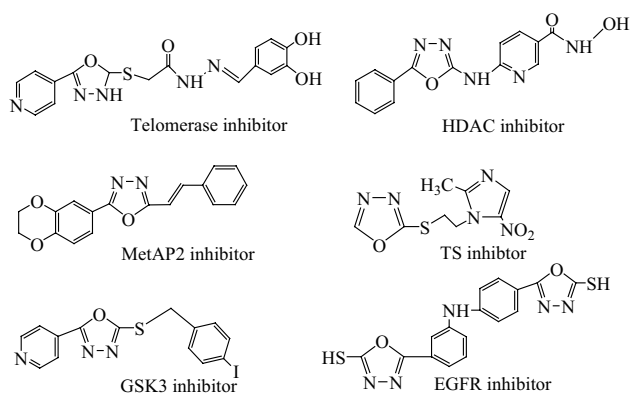


**Fig. 1** Structure of some representative bioactive compounds containing 1,3,4-oxadiazole moiety as anticancer agents

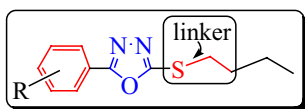
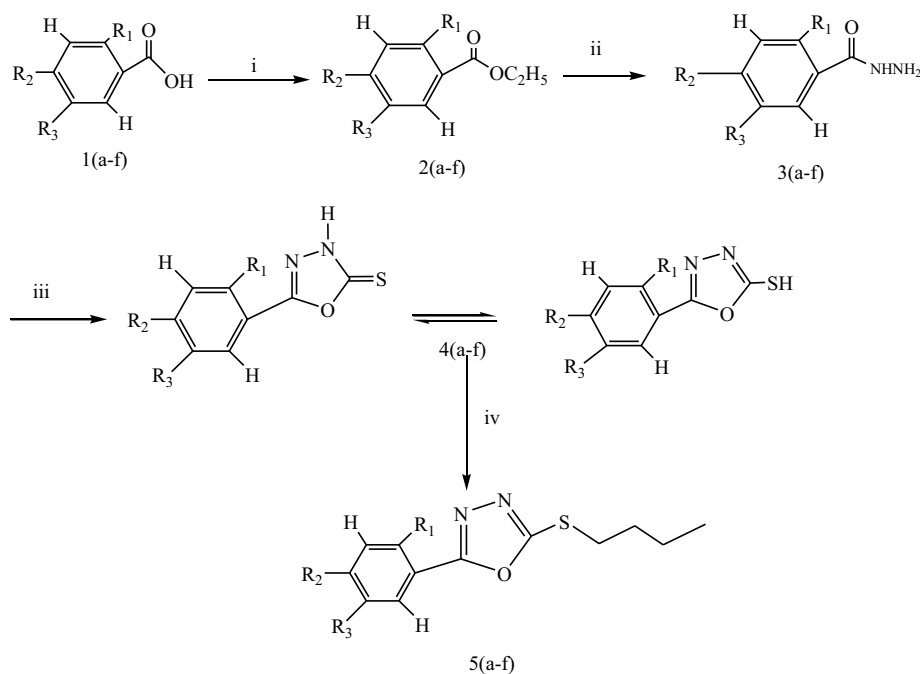


**Fig. 2** General structure of targeted compounds

**Scheme 1** Synthetic protocol for 5-aryl-2-(butylthio)-1,3,4-oxadiazole derivatives (**4a–5f**)



	R <sub>1</sub>	R <sub>2</sub>	R <sub>3</sub>
a.	H	H	H
b.	Cl	H	H
c.	Cl	Cl	H
d.	H	Tert-C <sub>4</sub> H <sub>9</sub>	H
e.	H	NH <sub>2</sub>	H
f.	Cl	H	NO <sub>2</sub>

**Reagents and Conditions** (i) ethanol, concentrated sulfuric acid; reflux, 8–12 h (ii) NH<sub>2</sub>NH<sub>2</sub>·H<sub>2</sub>O ethanol; reflux, 8–12 h (iii) (1) CS<sub>2</sub>/KOH, ethanol, reflux, 24 h; (2) HCl, pH 5–6; (iv) NaOH, acetonitrile, reflux, 8–24 h.

cells. Taking into consideration the therapeutic importance of 1,3,4-oxadiazole, we carried out the synthesis of new series of 5-aryl-2-butylthio-1,3,4-oxadiazole with objective to form promising anticancer agents (Fig. 2).

## Results and discussion

### Chemistry

Synthesis of the 5-aryl 2-butylthio-1,3,4-oxadiazole **5(a–f)** has been performed using the feasible chemical reactions outlined in Scheme 1. Acid hydrazide **3(a–f)**, a main intermediate in the formation of new oxadiazoles, was prepared by hydrazinolysis of **2(a–f)** with hydrazine hydrate in the presence of absolute alcohol by reported protocol [19]. 2,5-Disubstituted-1,3,4-oxadiazole was synthesized as previously reported [20] from intramolecular cyclization of **3(a–f)** using CS<sub>2</sub> and KOH in the presence of ethanol, followed by acidification. The synthesis of final compounds 5-aryl 2-butylthio-1,3,4-oxadiazole was accomplished by refluxing

equimolar mixture of **4(a–f)**, with 1-iodobutane in the presence of NaOH using acetonitrile as solvent. Data obtained from various spectroscopic techniques such as FTIR, <sup>1</sup>HNMR, <sup>13</sup>CNMR and ESI–MS provide structural confirmation of all target compounds. Purity was assessed using elemental analyses. When compound **3(a–f)** was converted to the corresponding 1,3,4-oxadiazoles **4(a–f)**, the absorption bands appeared in IR spectra due to –NH/NH<sub>2</sub> and –NHCO group disappeared instead, new absorption bands due to NH, C=N, –SH, –C–O–C appeared at 3264, 1602, 2557, 1324 and 1163 cm<sup>-1</sup>, respectively. <sup>1</sup>HNMR spectra of compounds **4(a–f)** were confirmed by the appearance of a new broad signal at δ 14.95 representing thiol–thione tautomerism while signals obtained in range of δ 7.86–δ 7.45 correspond to aromatic protons. *J* values were shown to be in concurrence with various substitutions present on the phenyl ring. For <sup>13</sup>CNMR spectra of compounds **4(a–f)**, C-2 carbon showed up field chemical shift at δ 177.53 while C-5 at δ 161.15 as C-2 carbon is directly attached with sulfur. The carbon C-1 of phenyl ring attached directly to 1,3,4-oxadiazole ring appeared at δ 122.93, while the peaks at δ 126.54, 128.30, 131.69, 133.54, 137.72 and 138.92 correspond to the phenyl ring. In general, for final compounds **5(a–f)**, NH and C=S groups which showed the sharp stretching band at 3266, 1234 cm<sup>-1</sup>, respectively, for compounds (**4a–f**) vanished signifying *S*-alkylation. Also the <sup>1</sup>HNMR spectra of compounds **5(a–f)** showed the presence of new signals at δ 3.33–3.19 due to –SCH<sub>2</sub> representing the formation of *S*-alkyl derivative. Further, in <sup>13</sup>CNMR spectrum of final compounds **5(a–f)**, the signal at δ 177.13 due to C=S was missing. Conversely, compound **4(a–f)** showed its presence which is the strong evidence for *S*-alkylation. Further, mass spectra of **4(a–f)** and **5(a–f)** compounds confirmed their molecular ion peaks at *m/z* (see supplementary data).

## Pharmacology

### *In vitro* inhibition of cell growth by 5-aryl-2-butylthio-1,3,4-oxadiazoles

All the synthesized compounds 5-aryl-2-thio-1,3,4-oxadiazoles **4(a–f)** and 5-aryl-2-butylthio-1,3,4-oxadiazoles **5(a–f)** were screened for their inhibitory growth effect on breast (MCF-7) and liver (HepG-2) human cancer cell lines using 3-(4,5-dimethylthiazol-2-yl)-2,5-diphenyltetrazolium bromide (MTT) assay [4]. To further explore the toxicity and selectivity, the cytotoxic evaluation against normal human embryonic cell line (HEK-293) was carried out for all synthesized compounds. Doxorubicin was used as the reference drug in the assay. The IC<sub>50</sub> (μM) values (concentration required to inhibit cancer cells growth by 50% after 48 h incubation) for both tested compounds and reference drug (Doxorubicin) have been shown in Table 1.

The results of *in vitro* studies revealed that few synthesized compounds were potentially successful in inhibiting cell growth of MCF-7 cancer cell having IC<sub>50</sub> values in range of 10.05 ± 1.08 μM to 18.79 ± 2.13 μM.

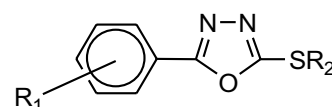
From close observation of IC<sub>50</sub> values, it is noticed that among all the compounds, **4e**, **4f**, **5e** and **5f** were more active having IC<sub>50</sub> values less than 25 μM on MCF-7 cancer cell line. It was observed that the compound **5e** during cell growth showed highest growth inhibition on MCF-7 cancer cell line with IC<sub>50</sub> value of 10.05 ± 1.08 μM which is less than standard drug Doxorubicin (IC<sub>50</sub> value 19.53 ± 1.50 μM). Since compound **5e** was more sensitive for MCF-7 cells, thus signifying that the inhibition of growth may have occurred due to induction of apoptosis caused by compound **5e** in MCF-7 cells. Further, it was observed that a compound **5e** only was moderately active against HepG-2 cell line, while rest of all compounds did not exhibit any activity up to 100 μM.

All the synthesized compounds were further tested for toxicity against one normal human cell line (HEK-293); among all, compounds **4e**, **4f**, **5e** and **5f** which have IC<sub>50</sub> value ≤25 μM on MCF-7 cell line displayed high viability of cells indicating that these compounds were less toxic toward normal cells, thus showing definite selectivity between cancerous and normal cell than doxorubicin. Out of them, compound **5e** displayed moderate selectivity towards the MCF-7 and HepG-2 cancer cells where IC<sub>50</sub> was almost 26.7 and 5.5 fold higher in HEK-293, respectively, shown in (Figure S1) (supplementary data).

The selectivity indices were also measured for screening compounds. Compounds **5e** and **5f** showed good selectivity against MCF-7 and HEK-293 cell lines with the SI value more than 3 (Table 1). Higher SI value (>3) of a compound represents more selectivity and toxicity towards cancer cells. Whereas SI value <3 exhibits moderate toxicity; however, it also increases cytotoxicity for normal cells [21]. The observed values of selectivity indices for compounds **4e**, **4f**, **5d** and **5f** were found to be 10.97, 9.70, 26.70 and 16.96, respectively, on breast cancer cell line MCF-7. Thus, from observations it was concluded that the synthesized compounds showed significant results on MCF-7 cell line as compared to HepG-2 cell line.

### Structure–activity relationship (SAR) of synthesized compounds (**4a–5f**)

On analyzing the MTT assay results, it was observed that the MCF-7 cells were found to be more sensitive towards synthesized target compounds. The effect of substituents “R<sub>1</sub>” on phenyl ring at C-5 carbon and the presence of butyl chain at C-2 carbon of 1,3,4-oxadiazole scaffold were important in analyzing SAR study. On comparing both series, compounds substituted with butyl linkage (**5a–5f**) were found

**Table 1** Selectivity index (SI) and IC<sub>50</sub> values of compounds on HEK-293, MCF-7 and Hep G-2

2,5-Disubstituted 1,3,4-oxadiazole

Compound no.	R	HEK-293 <sup>a</sup>	MCF-7 <sup>b</sup>		HepG-2 <sup>c</sup>	
		IC <sub>50</sub> (μM) ± SD	IC <sub>50</sub> (μM) ± SD	SI <sup>d</sup>	IC <sub>50</sub> (μM) ± SD	SI
<b>4a</b>	R <sub>1</sub> = H; R <sub>2</sub> = H	47.59 ± 1.00	53.01 ± 1.52	0.89	37.95 ± 1.52	1.23
<b>4b</b>	R <sub>1</sub> = Cl; R <sub>2</sub> = H	51.92 ± 0.95	41.85 ± 1.50	1.22	27.57 ± 1.84	1.79
<b>4c</b>	R <sub>1</sub> = Cl, Cl; R <sub>2</sub> = H	114.46 ± 2.00	55.69 ± 1.90	2.05	44.43 ± 1.60	2.57
<b>4d</b>	R <sub>1</sub> = tertbutyl; R <sub>2</sub> = H	51.14 ± 1.19	48.26 ± 1.50	1.05	38.96 ± 1.72	1.76
<b>4e</b>	R <sub>1</sub> = NH <sub>2</sub> ; R <sub>2</sub> = H	<b>183.31 ± 1.63</b>	<b>16.71 ± 2.11</b>	<b>10.97</b>	78.50 ± 1.67	2.33
<b>4f</b>	R <sub>1</sub> = Cl, NO <sub>2</sub> ; R <sub>2</sub> = H	<b>182.34 ± 1.51</b>	<b>18.79 ± 2.13</b>	<b>9.70</b>	84.75 ± 0.95	2.15
<b>5a</b>	R <sub>1</sub> = H; R <sub>2</sub> = <i>n</i> -butyl	51.82 ± 1.37	75.30 ± 1.82	0.68	55.70 ± 1.50	0.93
<b>5b</b>	R <sub>1</sub> = Cl; R <sub>2</sub> = <i>n</i> -butyl	96.86 ± 2.05	37.21 ± 1.70	2.60	42.04 ± 1.49	2.30
<b>5c</b>	R <sub>1</sub> = Cl, Cl; R <sub>2</sub> = <i>n</i> -butyl	75.67 ± 1.84	37.60 ± 1.66	2.01	26.52 ± 1.56	2.85
<b>5d</b>	R <sub>1</sub> = tertbutyl; R <sub>2</sub> = <i>n</i> -butyl	70.02 ± 1.61	26.13 ± 1.56	2.82	35.16 ± 1.65	1.99
<b>5e</b>	<b>R<sub>1</sub> = NH<sub>2</sub>; R<sub>2</sub> = <i>n</i>-butyl</b>	<b>268.35 ± 1.66</b>	<b>10.05 ± 1.08</b>	<b>26.70</b>	80.30 ± 1.29	3.34
<b>5f</b>	R <sub>1</sub> = Cl, NO <sub>2</sub> ; R <sub>2</sub> = <i>n</i> -butyl	<b>242.02 ± 1.09</b>	<b>14.27 ± 1.51</b>	<b>16.96</b>	79.44 ± 1.08	3.04
Doxorubicin		140.20 ± 1.00	19.53 ± 1.50	7.17	19.80 ± 1.49	7.08

The bold values represent active compounds

<sup>a</sup> HEK293—normal human embryonic kidney cell line

<sup>b</sup> MCF7—breast cancer

<sup>c</sup> HepG2—liver cancer. No activity >100 μM. The values (in μM) represent the mean ± SE of three independent experiments

<sup>d</sup> Selectivity index (SI) = IC<sub>50</sub> of pure compound in a normal cell line/IC<sub>50</sub> of the same pure compound in cancer cell line, where IC<sub>50</sub> is the concentration required to inhibit 50% of the cell population

to be more potent than compounds containing free –SH group (**4a–4f**). Unsubstituted phenyl ring (**4a**) showed less inhibitory effects than compound having with substituted phenyl ring (**5a**). The presence of amino group appreciably contributed to the anticancer activity. In general, the compounds with strong electron donating group such as amino (**4e**, **5e**) at para-position of phenyl ring showed better inhibitory activity than those with electron withdrawing groups such as –Cl (**4b**, **5b**, **4c** and **5c**). Replacement of hydrogen atom with 3<sup>o</sup>-butyl group at para-position led to decrease in activity (**4d**, **5d**). Replacement with –Cl group at o-position led to a slight increase in activity (**4b**, **5b**); adding another –Cl group to para-position (**4c**, **5c**) further increased activity as compared to (**4b**, **5b**); however, it also increased the toxicity indicating that the addition of –Cl at para-position was not favored. Adding –NO<sub>2</sub> to meta-position along with –Cl at ortho significantly increased antitumor activity with decreased toxicity, indicating that the presence of electron withdrawing group at the meta-position of phenyl ring was favored.

The significant anticancer activity of compound **5e** on MCF-7 cells encouraged us to further study its effect at the cellular level, predominantly the mechanisms involved in inhibition of cell growth.

#### *In silico analysis of drug-like properties of designed compounds*

Using free services provided by Molinspiration server (<http://www.molinspiration.com>), some of the physically and pharmaceutically important molecular properties based on Lipinski Rules of five were analyzed for all designed compounds as shown in Table 2. The entire sets of designed compounds showed no violations from the Lipinski's rule of five and possess all drugs-like properties [22].

#### *In vitro inhibition of cell migration by 5-(aminophenyl)-2-(butylthio)-1,3,4-oxadiazole (5e)*

Cell migration is important to various biological processes, specifically for cancer cells where migration

**Table 2** Molecular properties of compounds

Compounds	Milogp <5 no Desirable value	TPSA <140	No. of atoms –	MW <500	nON <10	nOHNH <5	Volume –	Nrotb <10
<b>4a</b>	2.32	38.92	12	178.22	3	0	146.37	1
<b>4b</b>	2.95	38.92	13	212.66	3	0	159.9	1
<b>4c</b>	3.61	38.92	14	247.11	3	0	173.44	1
<b>4d</b>	3.63	38.92	16	234.32	3	0	213.12	3
<b>4e</b>	1.40	64.95	13	193.23	4	2	157.66	1
<b>4f</b>	2.89	84.75	16	257.66	6	0	183.24	2
<b>5a</b>	3.97	38.92	16	234.32	3	0	213.80	5
<b>5b</b>	4.60	38.92	17	268.77	3	0	227.34	5
<b>5c</b>	5.25	38.92	18	303.21	3	0	240.87	5
<b>5d</b>	5.27	38.92	20	290.43	3	0	280.55	7
<b>5e</b>	3.04	64.95	17	249.34	4	2	225.09	5
<b>5f</b>	4.53	84.75	20	313.77	6	0	313.77	6

*MW* molecular weight, *nviolations* number of violations, *natoms* number of atoms, *nON* number of hydrogen bond acceptors, *nOHNH* number of hydrogen bond donors, *nrotb* number of rotatable bonds, *miLogP* log *P* value predicted by Molinspiration, *TPSA* topological polar surface area, *MV* molecular volume

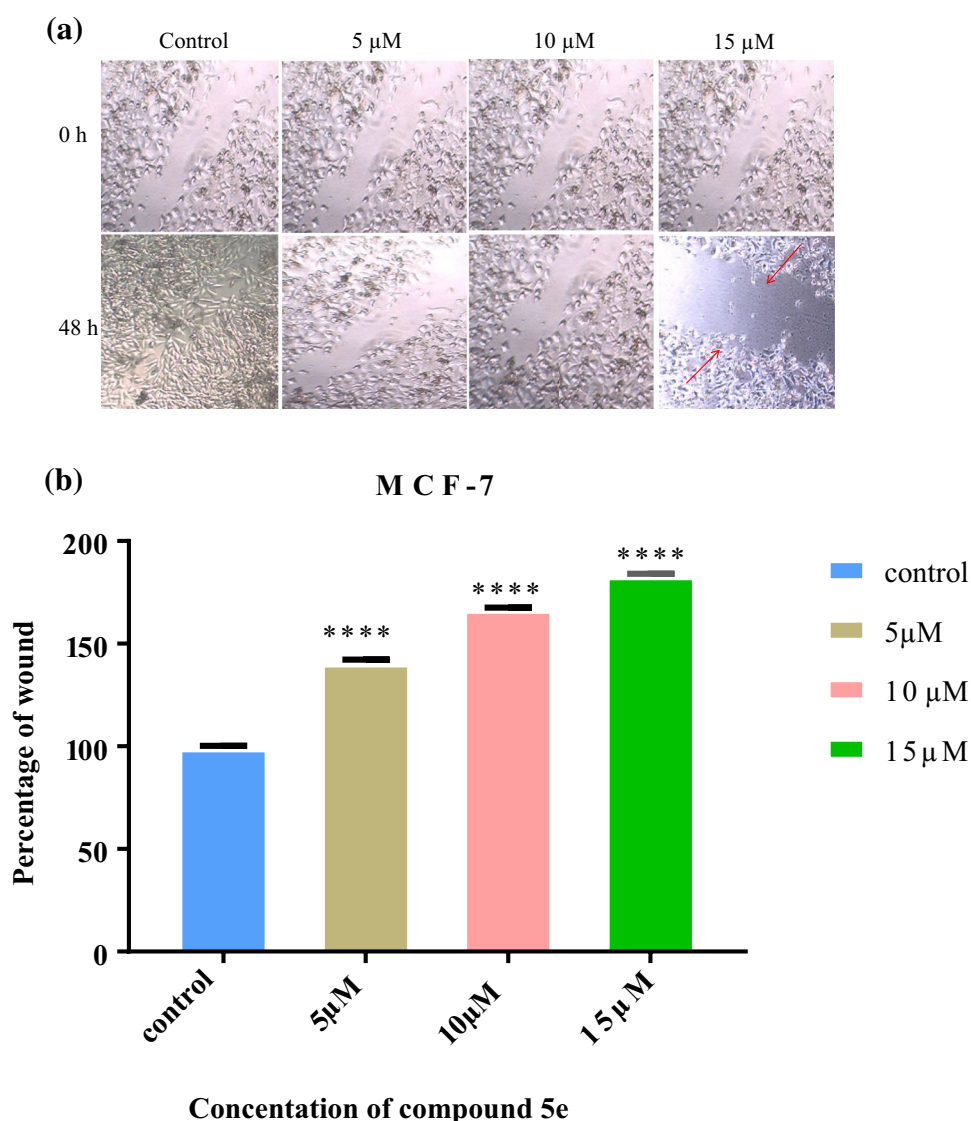
played a chief step in tumor progression and metastatic cascade [23]. The protocol for in vitro cell migration assay/wound healing assay is based on the fact that, when a new wound is formed artificially on a confluent cell monolayer, the cells present on the border of the freshly formed wound will migrate towards opening to cover up the wound till new cell–cell interaction formed. Movement of cells to cover up the wound can be restricted by treating cells with antitumor agent [24]. Thus, by carrying out in vitro cell migration assay, we have studied the outcome of the most active compound **5e** on the migration potential of cancerous MCF-7 cells. Wound was created on a confluent cell monolayer culture of MCF-7 cells using 200- $\mu$ L pipette tip and treated separately with 5, 10 and 15  $\mu$ M concentrations of compound **5e**. The migration of cancerous MCF-7 cells to cover up the wound on treatment with different concentrations of compound **5e** was observed and photographed after 48 h (Fig. 3a). The results showed that the width of wound increased efficiently on being treated with compound **5e**, whereas it decreased when remained untreated (control) for 48 h and scale bars were added to all images using ImageJ (Fig. 3b). The percentage of wound thickness for control and at 5, 10 and 15  $\mu$ M concentrations of **5e** compound was found to be 100, 141.36, 167.56 and 183.97%, respectively. These results revealed that migration of MCF-7 cancer cells was substantially suppressed by this derivative of 1,3,4-oxadiazole. All results were compared with control using unpaired *t* test and were shown

to be statistically significant with a level of significance ( $p < 0.0001$ ).

#### *Nuclear morphological changes using DAPI stain by 5-(aminophenyl)-2-(butylthio)-1,3,4-oxadiazole (5e)*

DAPI (4',6-diamidino-2-phenylindole) is a fluorescent dye which firmly binds with A-T rich region in DNA and also identifies the nuclear damage or condensation of chromatin. DAPI cannot pass through the membrane of live cells very effectively; thus, the stain is not so effective in live cells. Due to the condensed nucleus, the apoptotic cells appeared as bright colored on staining with DAPI; this is a distinctive characteristic of apoptosis [25]. Hence, we studied the effect of compound **5e** in MCF-7 cells by using DAPI staining assay, which distinguishes live cells from apoptotic cells based on nuclear morphology. As observed from Fig. 4a, the nuclear structure of control cells remains intact while morphological changes of cells were observed after treatment was done for 48 h with 5, 10 and 15  $\mu$ M concentrations of compound **5e**. The percentage of apoptotic cell at 5, 10 and 15  $\mu$ M concentrations of compound **5e** was found to be 68.57, 77.14 and 88.57%, respectively (Fig. 4b). When the cells had treated with increasing concentrations of compound **5e**, the total number of apoptotic cells was increased. All results were shown to be statistically significant and compared with control using unpaired *t* test with a level of significance ( $p < 0.0001$ ).

**Fig. 3** In vitro cell migration assay: **a** MCF-7 cells were treated with compound **5e** (5, 10 and 15  $\mu\text{M}$ ) and artificial scratches were done with sterile 200 mL pipette. The images were at photographed 0 and 48 h. **b** The rate of wound closure was photographed after 48 h and *scale bars* were added to images using ImageJ. Figure shows that the width of the wound increased effectively after the treatment with 5, 10 and 15  $\mu\text{M}$  concentrations of compound **5e** for 48 h in MCF-7 cell lines \*\*\*\* $p < 0.0001$  versus controls



*Measurement of reactive oxygen species (ROS) using NBT reduction assay by 5-(aminophenyl)-2-(butylthio)-1,3,4-oxadiazole (5e)*

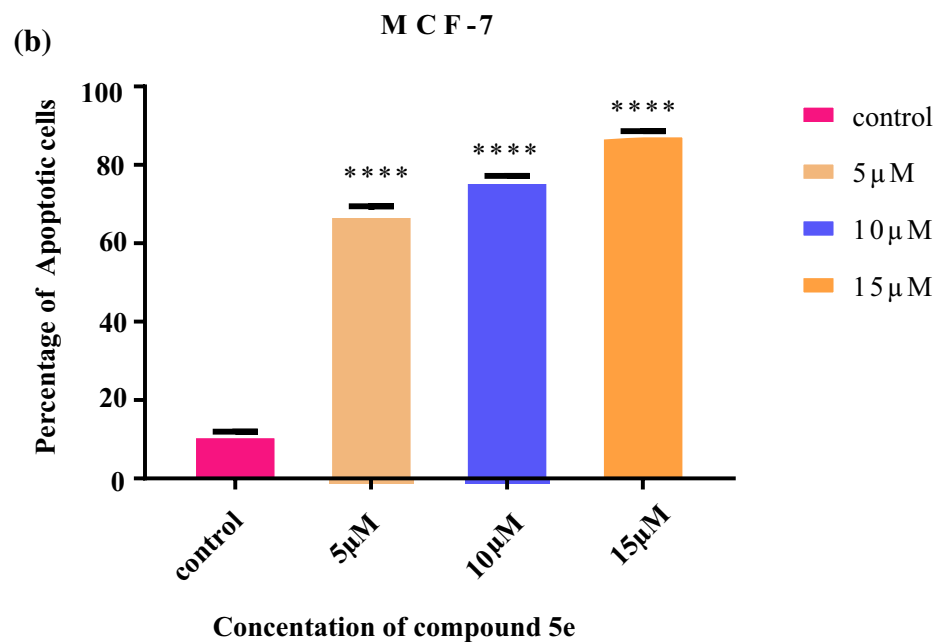
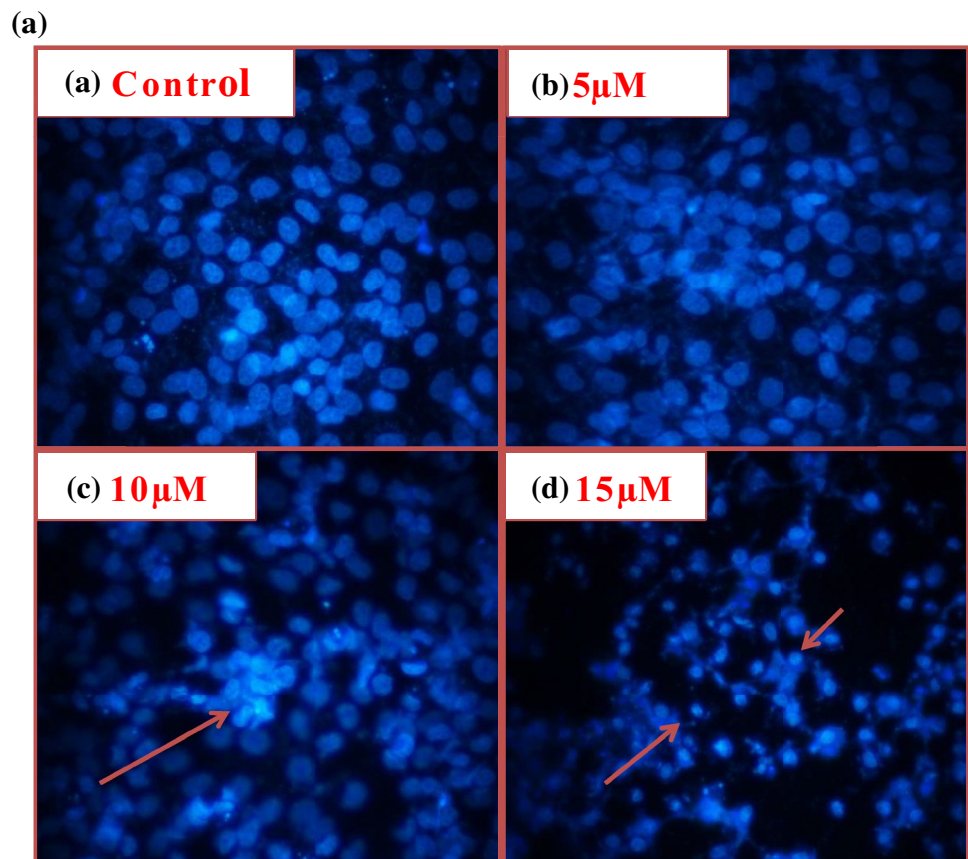
The reactive oxygen species generation is an important characteristic of many anticancer drugs as they regulate various biological processes such as cell proliferation, cell death and signaling [26]. Therefore, we evaluated the generation of ROS by compound **5e** in MCF-7 cells using NBT assay. Colorimetric nitro blue-tetrazolium (NBT) assay involves selective reduction in yellow water-soluble tetrazolium chloride by superoxide to an insoluble violet di-formazan [27]. We assessed the reduction in NBT by treating with 5, 10 and 15  $\mu\text{M}$  concentrations of compound **5e**. The results have revealed that the level of NBT on MCF-7 cells reduced from 92.68% (Doxorubicin) to 85.6% (**5e**) at 2.5  $\mu\text{M}$ ; 82.29% (Doxorubicin) to 69.29% (**5e**) at 5  $\mu\text{M}$ ; 67.24%

(Doxorubicin) to 55.96% at 10  $\mu\text{M}$  and 55.23% (Doxorubicin) to 43.9% (**5e**) at 15  $\mu\text{M}$ . Therefore, MCF-7 cells on treatment with increasing concentration of **5e** compound could remarkably result in a reduction in NBT as compared to standard (Doxorubicin) (Fig. 5). All results were shown to be statistically significant and compared with standard using unpaired *t* test with a level of significance ( $p < 0.0001$ ).

*Inhibition of cell growth using cell cycle analysis by 5-(aminophenyl)-2-(butylthio)-1,3,4-oxadiazole (5e)*

Inhibition of cell growth by arresting cell cycle at a certain specific checkpoint is a characteristic property exhibited by anticancer compounds [28]. Thus, obstructing the progression of the cell cycle using chemotherapeutic agents has become the most significant approach for developing antitumor therapeutics. In vitro screening results showed

**Fig. 4** Nuclear morphology of MCF-7 cells after DAPI staining. **a** Cells were treated with different concentrations of compound **5e** for 48 h and stained with DAPI. The control represents DAPI stain of MCF-7 cells without **5e** treatment. The images were captured with fluorescence microscope. **b** Histogram representation of the percentage of total and observed apoptotic cells against the different concentrations of compound **5e** for compounds on MCF-7 cancer cells. The control represents DAPI stain of MCF-7 cells without **5e** treatment \*\*\*\* $p < 0.0001$  versus controls



that the compound **5e** had significant inhibitory growth effects against MCF-7 cells. Hence, we studied the effect of compound **5e** on MCF-7 cancer cells by analyzing the

distribution pattern of cells in different phases of cell cycle using flow cytometry [29]. MCF-7 cancer cells were treated with 5, 10 and 15  $\mu$ M concentrations of compound **5e** for

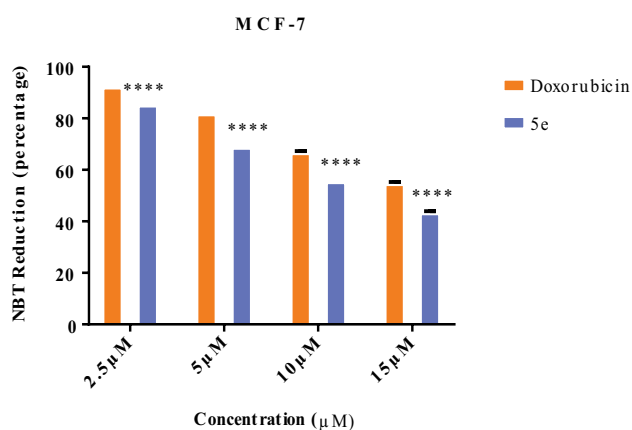


**Fig. 5** Compound **5e** reduced the ROS on the MCF-7 cells in a dose-dependent manner determined by the NBT reduction assay \*\*\*\* $p < 0.0001$  versus control

48 h; cells were then fixed in ethanol and stained with propidium iodide which were further analyzed by flow cytometry. The results from (Fig. 6a) showed that the ratio of MCF-7 cells increased for G0/G1 phase from 68.6% control (DMSO) to 73.2% at 5 µM, 73.3% at 10 µM and 73.8% at 15 µM concentrations of compound **5e**, respectively. Concomitantly, there was a decrease in the number of cells in both S and G2/M phases in a dose-dependent manner. However, the cell cycle analysis was not found so significant. Therefore, results from flow cytometry studies revealed that the treatment of MCF-7 cells with compound **5e** led to G0/G1 cell cycle arrest (Fig. 6b).

#### Apoptosis induction using Annexin-V/PE and 7-AAD binding assay by 5(aminophenyl)-2-(butylthio)-1,3,4-oxadiazole (**5e**)

In addition to further quantify the number of apoptotic cells after the treating with different concentrations of **5e**, annexin V-PE/7AAD dual staining analysis has been carried out [30]. The Annexin V-PE/7AAD binding assay identifies healthy cells (AV-/7AAD-), early apoptotic cells (AV+/7AAD-), late apoptotic cells (AV+/7AAD+) and complete dead cells (AV-/7AAD+). MCF-7 cells were treated with 5, 10 and 15 µM concentrations of compound **5e** for 48 h and stained using annexin V-PE and 7AAD. The results from Fig. 7 showed rise in the total percentage of apoptotic cells (early and late apoptotic cells) and dead cells from 4.7% (control) to 33.3% (5 µM), 34.14% (10 µM) and 71.3% (15 µM) concentrations of compound **5e**, respectively. The noteworthy increase in total percentage of (early and late apoptotic cells) and dead cells from 4.7 to 71.3% in a dose-dependent manner clearly signifies that the compound **5e** induced apoptosis in MCF-7 cells.

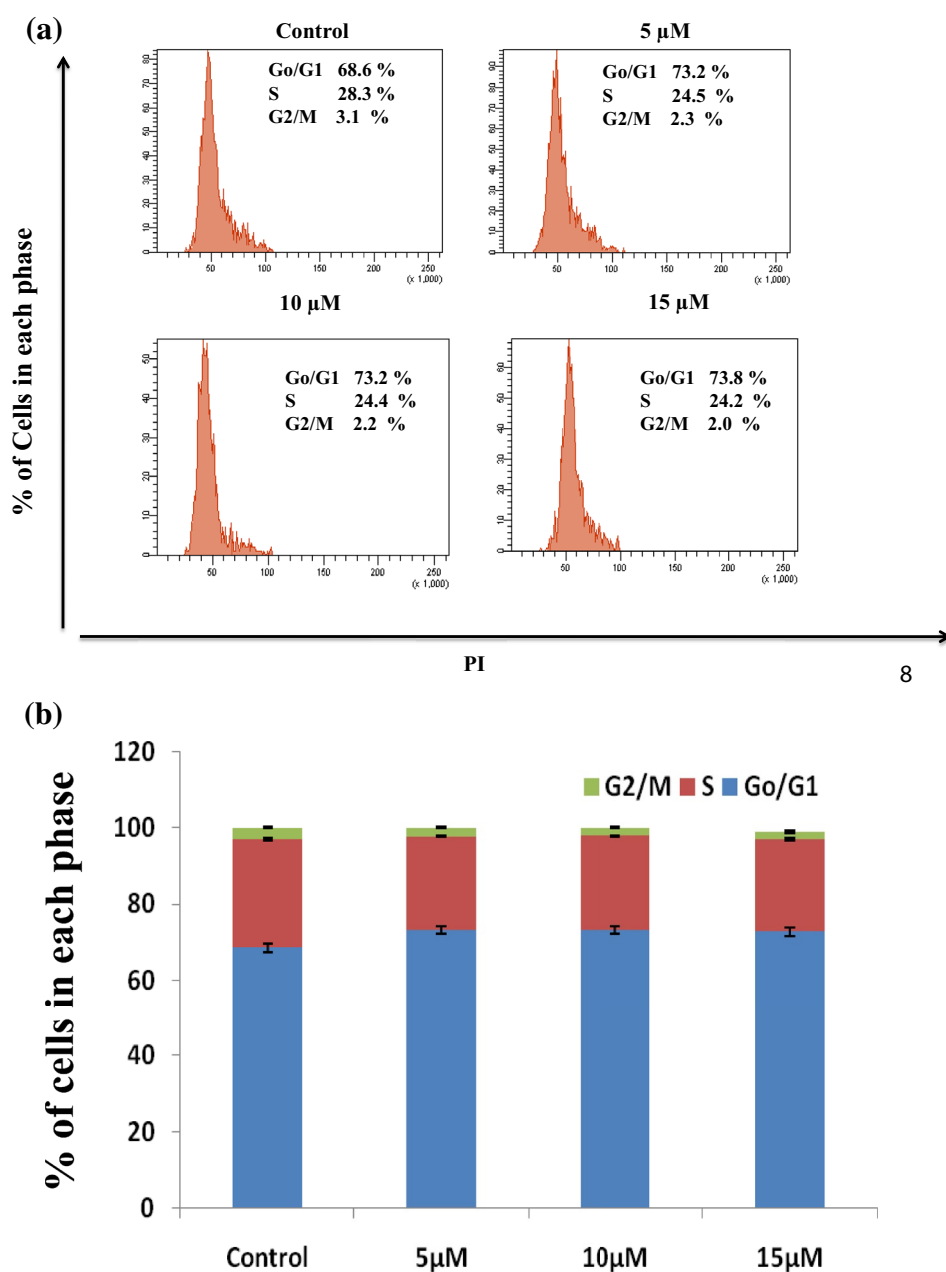
#### Western blotting analysis for apoptotic related proteins

Caspases and BCL-2 are some of the proteins whose expression plays a critical role in the apoptotic process. Particularly, caspase-3 is a member of cysteine-aspartic acid protease family which is known for catalyzing specific cleavage of many vital cellular proteins [31]. Therefore, to study the molecular mechanisms of compound **5e** on apoptosis, we have checked the expression of BCL-2 and caspase-3 on MCF-7 cancer cells using the western blot method [32]. As shown in Fig. 8, on being treated with 5, 10 and 15 µM concentrations of compound **5e** it led to the concentration-dependent increase in expression of caspase-3 in MCF-7 cells, which is a hallmark feature of apoptosis. Moreover, the compound **5e** treatment resulted in decreased expression of anti-apoptotic BCL-2 in a concentration-dependent manner. An increase in the expression of Caspase-3 and a decrease in BCL-2, respectively, were shown to be significant for MCF-7 cells. Therefore, these results illustrate that compound **5e** induced apoptosis through apoptosis-related protein expression.

#### Conclusion

A new series of 5-(aryl)-2-(butylthio)-1,3,4-oxadiazole has been synthesized and their cell growth inhibitory effect was estimated using in vitro MTT assay on human cancer cell lines MCF-7 (breast) and HepG-2 (liver) along with the normal kidney embryonic cell line (HEK-293). The screening results showed that a few of the synthesized compounds showed significant inhibition of growth on MCF-7 cancer cell line with  $IC_{50}$  value less than 25 µM. Also, these compounds showed lesser cytotoxicity on normal kidney embryonic cells. All compounds exhibited good drug like properties in accordance with Lipinski's rule of five. Among all, compound **5e** showed the most significant inhibition of cell growth on MCF-7 cell line with  $IC_{50}$  value  $10.05 \pm 1.08$  µM. The exposure of MCF-7 cancer cells to compound **5e** resulted in in vitro inhibition of cell migration using the wound healing assay. The cell cycle analysis confirmed that the compound **5e** targets the G0/G1 phase of MCF-7 cells in a dose-dependent manner. Further investigation using DAPI staining and Annexin V-PE/7-AAD assays showed the compound **5e** induced apoptosis in MCF-7 cancer cells. NBT reduction assay of compound **5e** on MCF-7 cells led to the generation of superoxide ROS. Additionally, western blot analysis showed that dose-dependent treatment of compound **5e** on MCF-7 cancer cells led to increased expression of apoptotic protein caspase-3 and decreased expression of anti-apoptotic protein BCL-2. Based on the results of all studies, it could be concluded that 5-aminophenyl-2-butylthio-1,3,4-oxadiazole (**5e**) has the potential to be

**Fig. 6** Cell cycle analysis of MCF-7 cancer cells. **a** MCF-7 cells treated with compound (5, 10 and 15  $\mu$ M) for 48 h. The cell cycle distribution was performed using propidium iodide staining method and analyzed by flow cytometry FACSaria-III. **b** Data from 10,000 cells were collected for each data file. The percentage of cells in G<sub>0</sub>/G<sub>1</sub>, S and G<sub>2</sub>/M phase was quantified by means of Diva software



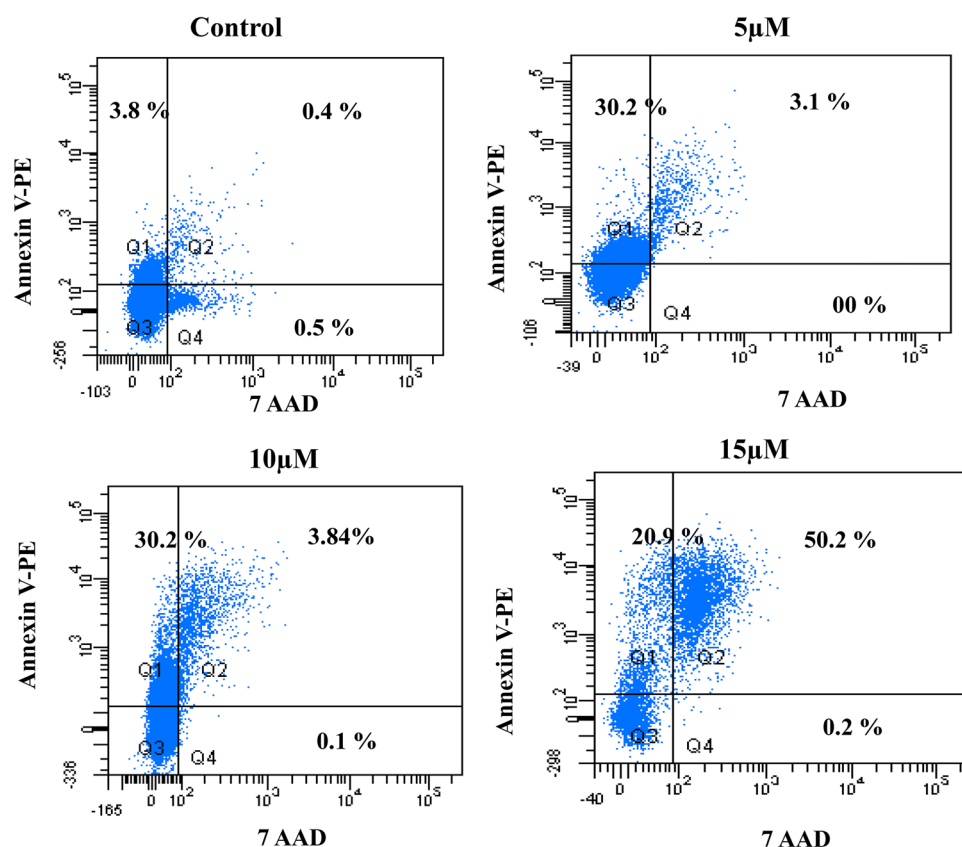
developed as lead molecule and further structural modifications may result in the development of new promising anti-cancer agents.

## Experimental

The acquisition of different chemicals and reagents had carried from Sigma-Aldrich, Merck (Germany) and had used without any further purification. Assessment and completion of the reaction were done analytically using aluminum precoated (silica gel 60 F254, Merck Germany) sheets by thin-layer chromatography (TLC) technique by

taking hexane/ethyl acetate in the ratio of (7.5:2.5) as eluting medium. Spots were visualized under UV light (256 nm). Using MEL-temp apparatus, melting points for all compounds were determined and the results were uncorrected. CHNS Elemental analyzer (Vario EL-III) had used to carry out elemental analysis of compounds and values so obtained were within range of  $\pm 0.3\%$  of calculated values. Bruker Tensor 37 FTIR spectrometer had used to obtain IR spectrum of all compounds and wave numbers were calculated in  $\text{cm}^{-1}$ . Bruker Advance 300 MHz spectrometer had used for obtaining NMR ( $^1\text{H}$  NMR and  $^{13}\text{C}$  NMR) spectra using MeOD/DMSO- $d_6$  as solvent. Taking tetramethylsilane as an internal reference,

**Fig. 7** Annexin V-PE/7-AAD dual staining assay. MCF-7 cells were treated with (5, 10 and 15  $\mu\text{M}$ ) concentrations compound **5e** and stained with Annexin V-PE/PI and analysed for apoptosis using flow cytometer



all chemical shift ( $\delta$ ) values were reported in parts per million (ppm) and coupling constant ( $J$ ) in Hertz while different abbreviations were used for specifying splitting pattern as follows: s, singlet; bs, broad singlet; d, doublet; t, triplet; q, quadruplet; m, multiplet. AB-Sciex 2000 had used for recording ESI-MS spectra. Spectral analysis data so obtained for all compounds had found to be in accordance with the proposed structure.

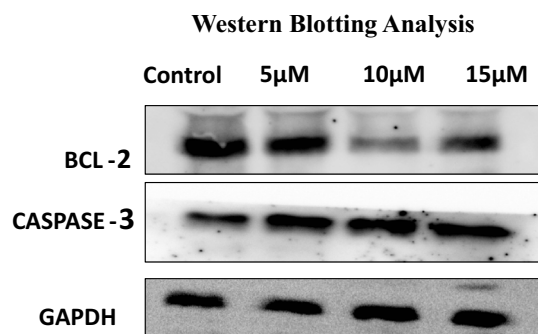


**Fig. 8** MCF-7 cells were treated with compound **5e** compound at (5, 10 and 15  $\mu\text{M}$ ) concentrations for 48 h and then the total protein extracts were analyzed using western blotting for BCL-2 and caspase-3

#### General procedure for synthesis of 5-(substituted benzyl)-1,3,4 oxadiazole-2-thione 4(a-f)

A solution of compounds **3(a-f)** (1 mmol) and  $\text{CS}_2/\text{KOH}$  (1 mmol) was taken in a mixture of ethanol/water in 1:1 ratio and refluxed for 15 h. With the help of TLC taking hexane: ethyl acetate (7.5:2.5) as mobile phase, the synthesis of reaction mixture had monitored. After reaction undergoes completion, its volume had reduced under pressure to half of its original volume. The reaction mixture was diluted with cold water and acidified with conc.HCL that resulted in the formation of solid precipitation. The product was filtered and the resulting precipitate was washed with water. Recrystallization was performed using methanol: dichloromethane (8:2) to obtain the desired product.

#### 5-(Phenyl)-1,3,4-oxadiazole-2-thione 4(a)

Yield = 61.9%; light brown crystal; mp = 135  $^\circ\text{C}$ ;  $R_f$  = 0.270 [hexane: ethyl acetate (7.5: 2.5)]; IR  $\nu_{\text{max}}$  ( $\text{cm}^{-1}$ ): 3264 ( $-\text{NH}$ ), 1604 ( $-\text{C}=\text{N}$ ), 1232 ( $-\text{C}=\text{S}$ ), 1326, 1164 ( $-\text{C}-\text{O}-\text{C}$ ):  $^1\text{H}$ NMR ( $\text{DMSO}-d_6$ , 300 MHz, ppm):  $\delta$  14.75 (s, 1H, thiol-thione tautomerism), 7.89–7.56 (m, 5H);  $^{13}\text{C}$ NMR ( $\text{DMSO}-d_6$ , 300 MHz, ppm):  $\delta$  177.97, 161.15, 133.10, 132.71, 130.06, 129.86, 127.04, 122.93; Elemental analysis

(calc.) for  $C_8H_6N_2OS$  (%): C, 53.91 (53.92); H, 3.38 (3.39); N, 15.71 (15.72); S, 17.93 (17.99); mass  $m/z$  ( $M^+$ ) 179.4.

**5-(2-Chlorophenyl)-1,3,4-oxadiazole-2-thione 4(b)**

Yield = 63.3%; white crystal; mp = 145 °C;  $R_f$  = 0.160 [hexane: ethyl acetate (7.5:2.5)]; IR  $\nu_{max}$  ( $cm^{-1}$ ): 3222 (–NH), 1612 (–C=N), 1231 (–C=S), 1321, 1163 (–C–O–C), 788 (–C–Cl);  $^1H$ NMR (DMSO- $d_6$ , 300 MHz, ppm):  $\delta$  14.91 (s, 1H, thiol–thione tautomerism), 7.92–7.90 (m, 1H), 7.71–7.60 (m, 1H), 7.66–7.62 (m, 1H), 7.57–7.54 (m, 1H);  $^{13}C$ NMR (DMSO- $d_6$ , 300 MHz, ppm):  $\delta$  177.25, 158.40, 133.30, 131.52, 131.16, 130.74, 127.80, 121.31; Anal found (calc.) for  $C_8H_5ClN_2OS$  (%): C, 45.21 (45.21); H, 2.37 (2.46); N, 13.17 (12.30); S, 17.44 (15.08); mass  $m/z$  ( $M + 2$ ) 212.6.

**5-(2,4-Dichlorophenyl)-1,3,4-oxadiazole-2-thione 4(c)**

Yield = 67.7%; yellow crystal; mp = 152 °C;  $R_f$  = 0.145 [hexane: ethyl acetate (7.5: 2.5)]; IR  $\nu_{max}$  ( $cm^{-1}$ ): 3267 (–NH), 1601 (–C=N), 1233 (–C=S), 1321, 1163 (–C–O–C), 789 (–C–Cl);  $^1H$ NMR (DMSO- $d_6$ , 300 MHz, ppm):  $\delta$  14.724 (s, 1H, thiol–thione tautomerism), 7.88–7.85 (d,  $J$  = 8.3, 1H), 7.77–0.76 (d,  $J$  = 8.2 Hz, 1H), 7.59–7.56 (m, 1H);  $^{13}C$ NMR (DMSO- $d_6$ , 300 MHz, ppm):  $\delta$  177.52, 158.19, 137.72, 133.01, 132.23, 131.24, 128.56, 120.73; Anal found (calc.) for  $C_8H_4Cl_2N_2OS$  (%): C, 37.71 (38.89); H, 1.63 (1.86); N, 11.34 (10.29); S, 12.98 (13.17); mass  $m/z$  ( $M + 2$ ) 249.1.

**5-(4-tertbutylphenyl)-1,3,4-oxadiazole-2-thione 4(d)**

Yield = 63.3%; yellow crystal; mp = 142 °C;  $R_f$  = 0.251 [hexane: ethyl acetate (7.5: 2.5)]; IR  $\nu_{max}$  ( $cm^{-1}$ ): 3264 (–NH<sub>2</sub>), 1605 (–C=N), 1222 (–C=S), 1342, 1167 (–C–O–C);  $^1H$ NMR (DMSO- $d_6$ , 300 MHz, ppm):  $\delta$  14.60 (s, 1H, thiol–thione tautomerism), 7.81–7.71 (m, 2H), 7.50–7.39 (m, 2H), 4.24–4.22 (d, 2H), 1.42–1.0 (m, 1H);  $^{13}C$ NMR (DMSO,  $d_6$ , 300 MHz, ppm):  $\delta$  177.89, 165.97, 160.90, 156.44, 155.56, 129.39, 127.87, 125.73, 60.8, 14. Elemental analysis (calc.) for  $C_8H_7N_3OS$  (%): C, 52.39 (49.73); H, 4.39 (3.65); N, 21.61 (21.75); S, 16.59 (16.25); MS (ESI): 1194.06.

**5-(4-Aminobenzyl)-1,3,4-oxadiazole-2-thione 4(e)**

Yield = 63.9%, mp = 146 °C;  $R_f$  = 0.23 [hexane: ethyl acetate (7.5:2.5)]; IR  $\nu_{max}$  ( $cm^{-1}$ ): 3278 (–NH<sub>2</sub>), 3010 (–C(CH<sub>3</sub>)<sub>3</sub>), 1614 (–C=N), 1256 (–C=S), 1340, 11,789 (–C–O–C);  $^1H$ NMR (DMSO- $d_6$ , 300 MHz, ppm):  $\delta$  14.609 (s, 1H, thiol–thione tautomerism), 7.80–7.78 (m, 2H), 7.51–7.42 (m, 2H), 5.9 (s, 2H);  $^{13}C$ NMR (DMSO- $d_6$ ,

300 MHz, ppm):  $\delta$  177.8, 165.97, 160.90, 156.44, 155.56, 129.39, 127.82, 127.62, 126.54, 126.26, 125.73, 125.2. Elemental analysis (calc.) for  $C_{12}H_{14}N_2OS$  (%): C, 60.52 (60.51); H, 5.60 (5.62); N 10.03 (11.96); S, 18.14 (18.68); MS (ESI): 235.08.

**5-(2-Chloro-5-nitrobenzyl)-1,3,4-oxadiazole-2-thione 4(f)**

Yield = 53.23%; brown crystal; mp = 177 °C;  $R_f$  = 0.187 [hexane: ethyl acetate (7.5: 2.5)]; IR  $\nu_{max}$  ( $cm^{-1}$ ): 3212 (–NH), 1657 (–C=N), 1266 (–C=S), 1344, 1178 (–C–O–C),  $^1H$ NMR (DMSO- $d_6$ , 300 MHz, ppm):  $\delta$  14.89 (s, 1H, thiol–thione tautomerism), 7.92 (s, 1H), 7.65–7.63 (d,  $J$  = 8.1, 1H), 7.62–7.61 (d, 1H);  $^{13}C$ NMR (DMSO- $d_6$ , 300 MHz, ppm):  $\delta$  175.45, 160.34, 138.34, 136.78, 134.67, 132.33, 128.83, 126.34. Anal found (calc.) for  $C_8H_4ClN_3O_3S$  (%): C, 39.9 (37.29); H, 2.31 (1.56); N, 15.98 (16.31); S, 12.46 (12.45).

**General procedure for preparation of 5-(substituted benzyl)-2-butylthio-1, 3, 4-oxadiazole 5(a–f)**

1 mmol of compounds **4(a–f)** and 1 mmol of NaOH were mixed and stirred in 20 mL of acetonitrile. To the above mixture, 1 mmol of 1-iodobutane dissolved in 5 mL of acetonitrile was added dropwise continuously with stirring. The reaction mixture had left on reflux for 24 h. TLC had used taking hexane: ethyl acetate (7.5:2.5) as mobile phase to access the progress of reaction mixture. The solution had allowed cooling to room temperature and excess of solvent had distilled off under pressure. The residue was diluted using ethyl acetate and washed with saturated brine thrice. The organic layer had separated and dried over anhydrous Na<sub>2</sub>SO<sub>4</sub>, filtered and the solvent had finally distilled off. Recrystallization was done from methanol to afford desired products **5(a–f)**.

**2-(Butylthio)-5-(phenyl)-1,3,4-oxadiazole 5(a)**

Yield = 51.2%; mp = 105 °C;  $R_f$  = 0.375 [hexane: ethyl acetate (7.5: 2.5)]; IR  $\nu_{max}$  ( $cm^{-1}$ ): 3313 (C–H, Ar–H), 1657 (–C=N), 1266 (–C=S), 1344, 1178 (–C–O–C);  $^1H$ NMR (DMSO- $d_6$ , 300 MHz, ppm):  $\delta$  7.86–7.41 (m, 5H), 3.22–3.17 (t, 2H), 1.45–1.41 (m, 2H), 1.38–1.31 (m, 2H), 0.94–0.90 (t, 3H);  $^{13}C$ NMR (DMSO- $d_6$ , 300 MHz, ppm):  $\delta$  158.15, 134.10, 133.71, 131.06, 128.86, 126.04, 123.162, 31.811, 29.3, 12.698; Elemental analysis (calc.) for  $C_{12}H_{14}N_2OS$  (%): C, 61.51 (61.52); H, 6.02 (6.04); N, 11.96 (11.92); S, 13.68 (13.67); mass  $m/z$  ( $M^+$ ) 235.09.

*5-(2-Chlorophenyl)-2-(butylthio)-1,3,4-oxadiazole 5(b)*

Yield = 85.2%; mp = 116 °C;  $R_f$  = 0.156 [hexane: ethyl acetate (7.5: 2.5)]; IR  $\nu_{\max}$  ( $\text{cm}^{-1}$ ): 3313 (C–H, Ar–H), 1657 (–C=N), 1266 (–C=S), 1344, 1178 (–C–O–C), 778 (C–Cl);  $^1\text{H}$ NMR (DMSO- $d_6$ , 300 MHz, ppm):  $\delta$  7.83–7.80 (m, 1H), 7.78–7.76 (m, 1H), 7.45–7.40 (m, 1H) 3.24–3.19 (t, 2H), 1.44–1.41 (m, 2H), 1.39–1.34 (m, 2H), 0.89–0.84 (t, 3H);  $^{13}\text{C}$ NMR (DMSO- $d_6$ , 300 MHz, ppm):  $\delta$  165.92, 163.90, 132.95, 132.44, 131.0, 130.77, 122.24, 31.83, 31.28, 31.28, 12.53; Elemental analysis (calc.) for  $\text{C}_{12}\text{H}_{12}\text{N}_2\text{OSCl}$  (%): C, 53.64 (53.62); H, 4.87 (4.88); N, 10.46 (10.42); S, 11.93 (11.94); mass  $m/z$  ( $M + 2$ ) 270.04.

*2-(Butylthio)-5-(2,4-dichlorophenyl)-1,3,4-oxadiazole 5(c)*

Yield = 56.2%; mp = 145 °C;  $R_f$  = 0.114 [hexane: ethyl acetate (7.5: 2.5)]; IR  $\nu_{\max}$  ( $\text{cm}^{-1}$ ): 3323 (C–H, Ar–H), 1654 (–C=N), 1268 (–C=S), 1178 (–C–O–C), 778 (C–Cl);  $^1\text{H}$ NMR (DMSO- $d_6$ , 300 MHz, ppm):  $\delta$  7.79–7.76 (d,  $J$  = 8.4, 1H), 7.51–7.49 (d,  $J$  = 8.1, 1H), 7.38–7.35 (m, 1H), 3.22–3.17 (t, 2H), 1.444–0.142 (m, 2H), 1.37–1.32 (m, 2H);  $^{13}\text{C}$ NMR (DMSO- $d_6$ , 300 MHz, ppm):  $\delta$  175.15, 165.59, 139.10, 134.56, 132.71, 131.06, 127.86, 126.04, 122.93, 33.18, 32.56, 31.67, 13.85; Elemental analysis (calc.) for  $\text{C}_{12}\text{H}_{12}\text{N}_2\text{ClOS}$  (%): C, 47.52 (47.52); H, 3.99 (3.98); N, 9.24 (9.23); S, 10.58 (10.54); mass  $m/z$  ( $M + 2$ ) 304.0.

*2-(Butylthio)-5-(p-tertbutylphenyl)-1,3,4-oxadiazole 5(d)*

Yield = 58.2%; mp = 107 °C;  $R_f$  = 0.1135 [hexane: ethyl acetate (8.5: 1.5)]; IR  $\nu_{\max}$  ( $\text{cm}^{-1}$ ): 3323 (C–H, Ar–H), 3200 ( $\text{NH}_2$ ) 1654 (–C=N), 1268 (–C=S), 1178 (–C–O–C);  $^1\text{H}$ NMR (DMSO- $d_6$ , 300 MHz, ppm):  $\delta$  7.85–7.67 (m, 2H), 7.54–7.40 (m, 2H), 4.28–4.26 (d, 2H), 4.055–4.033 (m, 6H), 3.41–3.23 (t, 2H), 0.93–0.89 (t, 3H);  $^{13}\text{C}$ NMR (DMSO- $d_6$ , 300 MHz, ppm):  $\delta$  156.15, 133.10, 132.71, 130.06, 128.86, 127.04, 121.93; Elemental analysis (calc.) for  $\text{C}_{12}\text{H}_{15}\text{N}_2\text{OS}$  (%): C, 57.81 (57.82); H, 6.69 (6.68); N, 16.84 (16.083); S, 12.86 (12.84); mass  $m/z$  ( $M^+$ ) 249.3.

*2-(Butylthio)-5-(p-aminophenyl)-1,3,4-oxadiazole 5(e)*

Yield = 48.6%; mp = 133 °C;  $R_f$  = 0.277 [hexane: ethyl acetate (7.5: 2.5)]; IR  $\nu_{\max}$  ( $\text{cm}^{-1}$ ): 3123 (C–H, Ar–H), 1613 (–C=N), 1216 (–C=S), 1168 (–C–O–C);  $^1\text{H}$ NMR (DMSO- $d_6$ , 300 MHz, ppm):  $\delta$  7.83–7.80 (m, 2H), 7.78–7.76 (m, 2H), 5.0 (s, 2H), 3.24–3.19 (t, 2H), 1.44–1.41 (m, 2H), 1.39–1.34 (m, 2H), 0.89–0.84 (t, 3H);  $^{13}\text{C}$ NMR (DMSO  $d_6$ , 300 MHz, ppm) 165.688, 165.096, 131.788, 129.029, 126.223, 125.91, 123.162, 31.87, 29.37, 12.69, 12.53; Anal found (calc.) for  $\text{C}_{16}\text{H}_{22}\text{N}_2\text{OS}$  (%): C, 66.17 (67.12); H, 7.64 (7.63); N 9.65 (9.64); S, 11.04 (11.04); mass  $m/z$  ( $M^+$ ) 291.43.

*2-(Butylthio)-5-(2-chloro-5-nitrophenyl)-1,3,4-oxadiazole 5(f)*

Yield = 42.6%; mp = 121.1 °C;  $R_f$  = 0.1937 [hexane: ethyl acetate (7.5: 2.5)]; IR  $\nu_{\max}$  ( $\text{cm}^{-1}$ ): 3133 (C–H, Ar–H), 1645 (–C=N), 1223 (–C=S), 1165 (–C–O–C);  $^1\text{H}$ NMR (DMSO- $d_6$ , 300 MHz, ppm):  $\delta$  7.79–7.76 (d, 1H), 7.51–7.49 (d, 1H), 7.38–7.35 (m, 1H), 4.73 (MeOD), 3.33–3.17 (t, 2H), 1.45–1.41 (m, 2H), 1.38–1.31 (m, 2H), 0.94–0.90 (t, 3H);  $^{13}\text{C}$ NMR (DMSO- $d_6$ , 300 MHz, ppm):  $\delta$  167.132, 164.30, 139.22, 134.56, 133.54, 131.04, 129.0, 122.42, 33.18, 32.188, 13.85, 11.60; Anal found (calc.) for  $\text{C}_{12}\text{H}_{12}\text{N}_3\text{O}_3\text{SCl}$  (%): C, 66.17 (67.12); H, 7.64 (7.63); N 9.65 (9.64); S, 11.04 (11.04); mass  $m/z$  ( $M^+$ ) 314.03.

**Pharmacological evaluations****Anticancer activity**

All the human cell lines including MCF-7 (breast cancer cell line), HepG-2 (Liver cancer cell line) and HEK-293 (normal Embryonic kidney cell line) used in these experiments had taken from NCCS (Pune, India). The cells had cultured in Roswell Park Memorial (RPMI) (Sigma Aldrich) containing 10% fetal bovine serum (Gibco-life technologies) along with 1% penicillin–streptomycin–neomycin in a humidified atmosphere having 5%  $\text{CO}_2$  maintained at 37 °C. On obtaining confluence of 80%, all the adherent cells were trypsinized using 0.25% of trypsin and re-suspended in medium supplemented with 10% FBS, 1% penicillin–streptomycin [33].

**Cytotoxicity assay**

MTT (3-(4,5-dimethylthiazol-2-yl)-2,5-diphenyltetrazolium bromide) assay was used to determine the cytotoxicity of cells through reduction in MTT by mitochondrial dehydrogenase to form thiazolyl blue formazan; the formazan so produced corresponds to the number of viable or active cell present in the medium [34]. 96-Well plate media were seeded with  $5 \times 10^3$  cells/well which contains 10% fetal bovine serum along with 1% penicillin–streptomycin and was then kept for overnight incubation time period at a humidified atmosphere containing 5%  $\text{CO}_2$  at 37 °C. The incubation media after keeping for 24 h had removed and to initiate serum starvation FBS-free media had added. Subsequently, the media were substituted with 200  $\mu\text{L}$  of completely fresh medium that consists of compounds and Doxorubicin in concentration range of 5–80  $\mu\text{M}$  for cancer cell lines and from 5 to 200  $\mu\text{M}$  for HEK 293. Doxorubicin was taken for reference standard drug (positive control). The supernatants after keeping for 48 h had removed and washing of cell was done with PBS. Then, adding 20  $\mu\text{L}$  of MTT solution

(5 mg/mL in PBS) to each well followed by 4 h of incubation in a humidified atmosphere chamber at 37 °C. The supernatant was removed from each well after 4 h. The colored formazan crystal so formed from MTT had mixed in 100 µL of DMSO and the absorbance had calculated at 570 nm wavelength using ELISA (enzyme linked immunoabsorbent assay reader (BioRad)) reader. The IC<sub>50</sub> values for all tested compounds had evaluated in Excel using best-fit regression curve method. All the experiments had been carried out in triplicate.

### Estimation of the selectivity index (SI)

The selectivity index corresponds to the ratio of IC<sub>50</sub> value calculated for the activity of synthesized compounds and standard drug on normal cell line HEK-293 to that of IC<sub>50</sub> calculated for cancer cell lines (MCF-7 and HepG-2). Values higher than three were considered to be optimum for an efficient selectivity index [21].

### In vitro wound healing assay (cell migration assay)

Cell migration assay was executed as described previously [35]. In short, cells were seeded in a 96-well plate and were left to grow overnight to the confluence. After keeping for 24 h, cultures had replaced with fresh medium carrying 0.5% FBS (control) and compound **5e** at their 5, 10 and 15 µM concentrations along with standard drug Doxorubicin. Monolayer cells had smashed with a 200-µL pipette tip to form a wound and kept in a 37 °C containing 95% air and 5% CO<sub>2</sub>. After keeping for 48 h, washing of cells had done twice with DMEM to take out floating cells. The rate of wound closure had estimated and photographed after 48 h, and scale bars had added to images using ImageJ.

### Fluorescence microscopic analysis of cell death (DAPI staining)

Fluorescence microscopy was used to observe cell nuclear morphology that had followed by 4',6-diamidino-2-phenylindole (DAPI) staining. The breast cancer MCF-7 cells had treated with fresh media (control) and also with 5, 10 and 15 µM concentrations of synthesized compound **5e** and Doxorubicin for 48 washing of cells had done with PBS (pH 7.4) followed by fixing with ice-cold 70% ethanol and suspended in 50 µL of DAPI (1 µg/mL DAPI in distilled water), and incubated for 20 min at 37 °C wrapped in aluminum foil. The cells had examined under Nikon Eclipse Ti fluorescence microscope. The following formula was used to calculate the percentage of apoptotic cells using the following formula [36].

$$\% \text{ of apoptotic cells} = \frac{\text{Total number of apoptotic cells}}{\text{Number of normal cells} + \text{Number of apoptotic cells}} \times 100.$$

### NBT reduction assay

Superoxide anion produced in cancer cells was determined by nitro blue tetrazolium (NBT) assay. NBT is a colorimetric assay which is conducted by figuring out the cells containing blue NBT formazan deposits, and this formazan is equivalent to the number of viable or active cells available in the medium [37]. 8 × 10<sup>3</sup> cells/well were seeded into the 96-well tissue culture plates, media having 10% FBS along with 1% penicillin–streptomycin and left for incubation at a temperature of 37 °C overnight. On completing 24 h, the incubation media were detached and FBS-free media and then added for starvation. The following day, media were changed with 200 µL of fully freshen medium consisting of concentration **5e** compound. Doxorubicin had taken as a standard reference drug (positive control) and its concentration ranging 2.5–15 µM for breast MCF-7 cancer cell lines was taken. After completion of 48 h, the supernatants taken off and washing of cells was then done with PBS and 100 µL of 0.1% NBT solution was added to each well, then the cells were incubated in a humidified atmosphere at 37 °C for 4 h. After 4 h, reduced NBT was then solubilized with 100 µL of DMSO along with 2 M KOH for another 30 min. The value of absorbance measured at 570 nm wavelengths using enzyme linked immunoabsorbent assay reader (ELISA) (BioRad). All experiments had repeated at least three times.

### Cell cycle analysis

MCF-7 cells were treated with 5, 10 and 15 µM concentrations of compound **5e** for 48 h. After treatment, cells were washed in PBS. Cells were then fixed in cold 70% ethanol and were added dropwise to the cell pellet while vortexing. Cells were fixed for at least 30 min at 4 °C. The cells were washed twice in PBS and were spin at 2000 rpm while maintaining and avoiding the cell loss when the supernatant was discarded, especially after spinning out of ethanol. To ensure that only DNA is stained, cells were treated with Ribonuclease. 50 µL of 100 µg/mL RNase was added. 200 µL of propidium iodide (50 µg/mL) was added. The samples were then analyzed for propidiumiodide fluorescence from 15,000 events by flow cytometry using BD Pharmingen flow cytometer [4].

### Annexin V-PE/7-AAD dual staining assay

The Annexin V-PE/7-AAD dual staining assay was carried out using reported protocol [4, 38]. The Annexin V-PE/7-AAD dual staining assay was carried out using MCF cells to quantify the percentage of apoptotic cells. MCF-7 cells were plated in six-well culture plates and grown for 48 h. After treating with increasing concentrations of compound **5e** (5,

10 and 15  $\mu\text{M}$ ) for 48 h, cells were collected by trypsinisation. The collected cells were washed two times with ice-cold PBS, and then incubated in binding buffer containing Annexin V-PE, and 7-AAD for 5 min at room temperature in the dark. After 15 min of incubation, cells were analyzed for apoptosis using BD Pharmingen flow cytometer.

### Western blotting analysis

Cells were grown in 10% FBS (Invitrogen), in DMEM (Life technologies) high gluco media with anti-(gibco) up to the 60% of the confluency. Compound was dissolved in the 100% ethanol and diluted up to the concentrations of 5, 10 and 15  $\mu\text{M}$  in the media. Cells were incubated for the 48 h in the  $\text{CO}_2$  incubator. Cells were washed by the ice cold PBS, and lysed using the lysis buffer (sigma) with the help of cell scrapper. Cell lysate was centrifuged at 13,000 rpm for 15 min at the 4 °C. Total cell protein was collected as the supernatant. Bradford reagent (G-Biosciences) was used for the protein estimation, using the BSA as the standard. 12% of the SDS-PAGE was run with 70  $\mu\text{g}$  of the total protein and transferred to the 0.4 micron PVDF (MDI) membrane. Then, membrane was blocked using the 5% BSA in TBST for 1 h. The blot was washed with TBST three times and incubated with primary antibody (1:1000) in 2% BSA in TBST for 12 h at the 4 °C. After 12 h, the primary antibodies were recovered and the blot was washed three times, each for 10 min with TBST. Then, the blot was incubated in secondary antibody (1:10,000) in 2% BSA in TBST for 1 h at the room temperature. The blot was washed by TBST, three times and developed using the ECL (G-bioscience) and Fujifilm LAS4000 chemiluminator. Further editing was done using the Fujifilm multiguage software. The primary antibodies used were anti-BCL2 (cell signaling technologies cat no. #2876) and anti-Caspase3 (Cell signaling technologies cat no. #9662) and anti-Rabbit (Cell signaling technologies cat no. #7074) were taken as secondary [38].

### Lipinski rules of five

We have analyzed some physically important descriptors and Drug like relevant properties of compounds based on Lipinski Rules of five, like log *P*, molecular weight, number of hydrogen bond acceptor and donor, using Molinspiration server (<http://www.molinspiration.com>) and ChemDraw software [39].

### Statistical analysis

Statistical analysis had performed using GraphPad Prism version 5.00. The results were expressed as mean value  $\pm$  SD

( $n = 3$ ). Statistical analysis was done by unpaired *t* test. Probability values of less than 0.0005 had considered significant.

**Acknowledgements** This research work had supported by UGC (F no-43-172/2014 (SR). Author Rashmin Khanam is grateful to UGC for providing NON-Net fellowship for financial support and Dr. Syed Shahabuddin for great help.

### Compliance with ethical standards

**Conflict of interest** The authors declare that they have no conflict of interest.

**Research involving human or animal participants** This article does not contain any studies with human participants or animals performed by any of the authors.

### References

1. Senwar KR, Reddy TS, Thummuri D, Sharma P, Naidu VG, Srinivasulu G, Shankaraiah N (2016) Design, synthesis and apoptosis inducing effect of novel (*Z*)-3-(3'-methoxy-4'-(2-amino-2-oxoethoxy)-benzylidene)indolin-2-ones as potential antitumour agents. *Eur J Med Chem* 118:34–46
2. George RF, Fouad MA, Gomaa IE (2016) Synthesis and cytotoxic activities of some pyrazoline derivatives bearing phenyl pyridazine core as new apoptosis inducers. *Eur J Med Chem* 112:48–59
3. Nagarsenkar A, Guntuku L, Guggilapu SD, Gannaju S, Naidu V, Bathini NB (2016) Synthesis and apoptosis inducing studies of triazole linked 3-benzylidene isatin derivatives. *Eur J Med Chem* 124:782–793
4. Sharma P, Thummuri D, Reddy TS, Senwar KR, Naidu VG, Srinivasulu G, Bhargava SK, Shankaraiah N (2016) New (*E*)-1-alkyl-1H-benzo[d]imidazol-2-yl)methylene)indolin-2-ones: synthesis, in vitro cytotoxicity evaluation and apoptosis inducing studies. *Eur J Med Chem* 122:584–600
5. Siegel R, Ma J, Zou Z, Jemal A (2014) Cancer statistics, 2014. *CA Cancer J Clin* 64:9–29
6. Fulda S (2009) Tumor resistance to apoptosis. *Int J Cancer* 124:511–515
7. Vashist A, Shahabuddin S, Gupta Y, Ahmad S (2013) Polyol induced interpenetrating networks: chitosan–methylmethacrylate based biocompatible and pH responsive hydrogels for drug delivery system. *J Mater Chem B* 1:168–178
8. Bajaj S, Asati V, Singh J, Roy PP (2015) 1,3,4-Oxadiazoles: an emerging scaffold to target growth factors, enzymes and kinases as anticancer agents. *Eur J Med Chem* 97:124–141
9. Zhang F, Wang XL, Shi J, Wang SF, Yin Y, Yang YS, Zhang WM, Zhu HL (2014) Synthesis, molecular modeling and biological evaluation of *N*-benzylidene-2-((5-(pyridin-4-yl)-1,3,4-oxadiazol-2-yl)thio)acetohydrazide derivatives as potential anticancer agents. *Bioorg Med Chem* 22:468–477
10. Valente S, Trisciuglio D, De Luca T, Nebbioso A, Labella D, Lenoci A, Bigogno C, Dondio G, Miceli M, Brosch G, Del Bufalo D, Altucci L, Mai A (2014) 1,3,4-Oxadiazole-containing histone deacetylase inhibitors: anticancer activities in cancer cells. *J Med Chem* 57:6259–6265
11. Du QR, Li DD, Pi YZ, Li JR, Sun J, Fang F, Zhong WQ, Gong HB, Zhu HL (2013) Novel 1,3,4-oxadiazole thioether derivatives targeting thymidylate synthase as dual anticancer/antimicrobial agents. *Bioorg Med Chem* 21:2286–2297

12. Gunosewoyo H, Midzak A, Gaisina IN, Sabath EV, Fedolak A, Hanania T, Brunner D, Papadopoulos V, Kozikowski AP (2013) Characterization of maleimide-based glycogen synthase kinase-3 (GSK-3) inhibitors as stimulators of steroidogenesis. *J Med Chem* 56:5115–5129
13. Zhang S, Luo Y, He LQ, Liu ZJ, Jiang AQ, Yang YH, Zhu HL (2013) Synthesis, biological evaluation, and molecular docking studies of novel 1,3,4-oxadiazole derivatives possessing benzotriazole moiety as FAK inhibitors with anticancer activity. *Bioorg Med Chem* 21:3723–3729
14. Cai ZW, Wei D, Borzilleri RM, Qian L, Kamath A, Mortillo S, Wautlet B, Henley BJ, Jeyaseelan R Sr, Tokarski J, Hunt JT, Bhide RS, Fargnoli J, Lombardo LJ (2008) Synthesis, SAR, and evaluation of 4-[2,4-difluoro-5-(cyclopropylcarbamoyl)phenylamino]pyrrolo[2,1-f][1, 2, 4]triazine-based VEGFR-2 kinase inhibitors. *Bioorg Med Chem Lett* 18:1354–1358
15. Yarden Y (2001) The EGFR family and its ligands in human cancer. Signalling mechanisms and therapeutic opportunities. *Eur J Cancer* 37(Suppl 4):S3–S8
16. Shahzad SA, Yar M, Bajda M, Jadoon B, Khan ZA, Naqvi SA, Shaikh AJ, Hayat K, Mahmood A, Mahmood N, Filipek S (2014) Synthesis and biological evaluation of novel oxadiazole derivatives: a new class of thymidine phosphorylase inhibitors as potential anti-tumor agents. *Bioorg Med Chem* 22:1008–1015
17. Chen H, Li Z, Han Y (2000) Synthesis and fungicidal activity against *Rhizoctonia solani* of 2-alkyl (alkylthio)-5-pyrazolyl-1,3,4-oxadiazoles (thiadiazoles). *J Agric Food Chem* 48:5312–5315
18. Agelis G, Resvani A, Koukoulitsa C, Tumova T, Slaninova J, Kalavrizioti D, Spyridaki K, Afantitis A, Melagraki G, Siafaka A, Gkini E, Megariotis G, Grdadolnik SG, Papadopoulos MG, Vlahakos D, Maragoudakis M, Liapakis G, Mavromoustakos T, Matsoukas J (2013) Rational design, efficient syntheses and biological evaluation of *N,N'*-symmetrically bis-substituted butylimidazole analogs as a new class of potent Angiotensin II receptor blockers. *Eur J Med Chem* 62:352–370
19. Husain A, Rashid M, Shaharyar M, Siddiqui AA, Mishra R (2013) Benzimidazole clubbed with triazolo-thiadiazoles and triazolo-thiadiazines: new anticancer agents. *Eur J Med Chem* 62:785–798
20. Liu K, Lu X, Zhang HJ, Sun J, Zhu HL (2012) Synthesis, molecular modeling and biological evaluation of 2-(benzylthio)-5-aryloxadiazole derivatives as anti-tumor agents. *Eur J Med Chem* 47:473–478
21. Fang SY, Tseng CC, Yang YL, Lee EJ, Chen HY, Bhardwaj A, Chen TY (2006) Nitric oxide scavenger carboxy-PTIO reduces infarct volume following permanent focal ischemia. *Acta Anaesthesiol Taiwan* 44:141–146
22. Morris GM (1998) Automated docking using a Lamarckian genetic algorithm and an empirical binding free energy function. *J Comput Chem* 19:1639–1662
23. Rodriguez LG, Wu X, Guan JL (2005) Wound-healing assay. *Methods Mol Biol* 294:23–29
24. Singh P, Bast F (2015) Screening of multi-targeted natural compounds for receptor tyrosine kinases inhibitors and biological evaluation on cancer cell lines, in silico and in vitro. *Med Oncol* 32:233
25. Shrivastava S, Jeengar MK, Reddy VS, Reddy GB, Naidu VG (2015) Anticancer effect of celastrol on human triple negative breast cancer: possible involvement of oxidative stress, mitochondrial dysfunction, apoptosis and PI3K/Akt pathways. *Exp Mol Pathol* 98:313–327
26. Zhang L, Zhang Z, Chen F, Chen Y, Lin Y, Wang J (2016) Aromatic heterocyclic esters of podophyllotoxin exert anti-MDR activity in human leukemia K562/ADR cells via ROS/MAPK signaling pathways. *Eur J Med Chem* 123:226–235
27. Singh P (2015) High-throughput virtual screening, identification and in vitro biological evaluation of novel inhibitors of signal transducer and activator of transcription 3. *Med Chem Res* 24(6):2694–2708
28. Chan KT, Meng FY, Li Q, Ho CY, Lam TS, To Y, Lee WH, Li M, Chu KH, Toh M (2010) Cucurbitacin B induces apoptosis and S phase cell cycle arrest in BEL-7402 human hepatocellular carcinoma cells and is effective via oral administration. *Cancer Lett* 294:118–124
29. Reddy TS, Kulhari H, Reddy VG, Bansal V, Kamal A, Shukla R (2015) Design, synthesis and biological evaluation of 1,3-diphenyl-1H-pyrazole derivatives containing benzimidazole skeleton as potential anticancer and apoptosis inducing agents. *Eur J Med Chem* 101:790–805
30. Praveen Kumar C, Reddy TS, Mainkar PS, Bansal V, Shukla R, Chandrasekhar S, Hugel HM (2016) Synthesis and biological evaluation of 5,10-dihydro-11*H*-dibenzo[*b, e*][1, 4]diazepin-11-one structural derivatives as anti-cancer and apoptosis inducing agents. *Eur J Med Chem* 108:674–686
31. Porter AG, Janicke RU (1999) Emerging roles of caspase-3 in apoptosis. *Cell Death Differ* 6:99–104
32. O'Brien MA, Moravec RA, Riss TL (2001) Poly (ADP-ribose) polymerase cleavage monitored in situ in apoptotic cells. *BioTechniques* 30:886–891
33. Syarifah MS (2011) Potential anticancer compound from *Cerbera odollam*. *J Tropic For Sci* 23:89–96
34. Mosmann T (1983) Rapid colorimetric assay for cellular growth and survival: application to proliferation and cytotoxicity assays. *J Immunol Methods* 65:55–63
35. Singh P, Bast F (2015) Screening of multi-targeted natural compounds for receptor tyrosine kinases inhibitors and biological evaluation on cancer cell lines, in silico and in vitro. *Med Oncol* 32:233
36. Ramar T (2012) A novel disintegrin protein from *Naja naja* venom induces cytotoxicity and apoptosis in human cancer cell lines in vitro. *Process Biochem* 47:1243–1249
37. Choi HS, Kim JW, Cha YN, Kim C (2006) A quantitative nitroblue tetrazolium assay for determining intracellular superoxide anion production in phagocytic cells. *J Immunoassay Immunochem* 27:31–44
38. Thummuri D, Jeengar MK, Shrivastava S, Areti A, Yerra VG, Yamjala S, Komirishetty P, Naidu VG, Kumar A, Sistla R (2014) *Boswellia ovalifoliolata* abrogates ROS mediated NF-kappaB activation, causes apoptosis and chemosensitization in Triple Negative Breast Cancer cells. *Environ Toxicol Pharmacol* 38:58–70
39. Lipinski CA, Lombardo F, Dominy BW, Feeney PJ (2001) Experimental and computational approaches to estimate solubility and permeability in drug discovery and development settings. *Adv Drug Deliv Rev* 46:3–26